Research Article

Three-Dimensional Tolerance Analysis and Allocation for Valve Gap of Engine

Yin Li[1], Hua Chen[2*] (ID)

[1]Shenzhen Softwin Technologies Co, Ltd. Songan RD, Bao'an District, Shenzhen, Guangdong, China
[2]Sino-German College of Intelligent Manufacturing, Shenzhen Technology University, 3002 Lantian RD, Pingshan District, Shenzhen, Guangdong, China
 Email: chenhua@sztu.edu.cn

Abstract: The engine is a typical complex machine with many mechanisms and high precision. The tolerance of the valve gap is an accumulative result of component tolerances in the valve mechanism, which is very critical to engine performance. The current tolerance analysis is carried out using the traditional linear dimension chain, and it is difficult to consider a large number of geometric tolerances. The analysis result is not consistent with reality. Based on an innovative three-dimensional tolerance model, i.e., the unified Jacobian-Torsor model, tolerance analysis and allocation for valve gap are presented in this paper, where large geometric and partial parallel connections are taken into consideration. For the special conical structure in the valve mechanism, the expression and variation of the conical torsor are deduced. At last, a real engine was selected as an example of the analysis process. Sufficient comparison and discussion were carried out for the results, which demonstrated the effectiveness of the method.

Keywords: Jacobian-Torsor model, tolerance analysis and allocation, valve gap, engine

1. Introduction

Internal combustion engines are the main source of power in modern society, pushing the great wheel of time forward. Meanwhile, the engine is a classic mechanical production, which contains a slider-crank mechanism, cam mechanism, gear mechanism, and so on. In the past few decades, although engines have made great achievements in combustion efficiency, emission level, and noise, vibration, and harshness (NVH), their basic structures have not changed much [1], [2]. However, this does not mean that the components of mechanical structures have not been improved, which are mainly reflected in materials and accuracy control. Because of its good thermal conductivity and lightweight, aluminum alloy gradually replaced cast iron as the main engine material [3]. As for accuracy control running through engine design, manufacturing, and measurement, it has been continuously improved and optimized [4].

The core of accuracy control is tolerancing, which can be classified into several categories, such as tolerance specification, tolerance analysis, tolerance allocation or synthesis, and so on [5]. Among them, tolerance analysis and allocation, which connect not only product performance but also their cost were closest to engineering applications [6]. Over the last decades, many tolerance analysis and allocation methods for engines have been proposed. Based on the state space equation, Wang et al. described variation propagation in multistage machining processes for cylinder blocks [7]. Yang et al. proposed a new error compensation model for the machining process based on differential motion

vectors [8]. By Monte Carlo simulation, Xu et al. carried out tolerance analysis and optimization for key structures of diesel engines [9]. Gong et al. used a linear method for tolerance analysis and optimization of the crank-linkage mechanism of engines. Using a Jacobian-Torsor model, Chen et al. attempted tolerance analysis and allocation for engines' mechanisms in a three-dimensional (3D) tolerance zone and took the partial parallel connections situation into consideration [10], [11]. The above methods are mainly aimed at tolerance analysis of the crank slider mechanism or error flow modeling of a single part of engines.

The valve system is composed of a camshaft, tappet, valve, cylinder head, and spring, as shown in Figure 1. The clearance between the cam and tappet is the valve gap, which is naturally formed after assembly and is essential for engine performance.
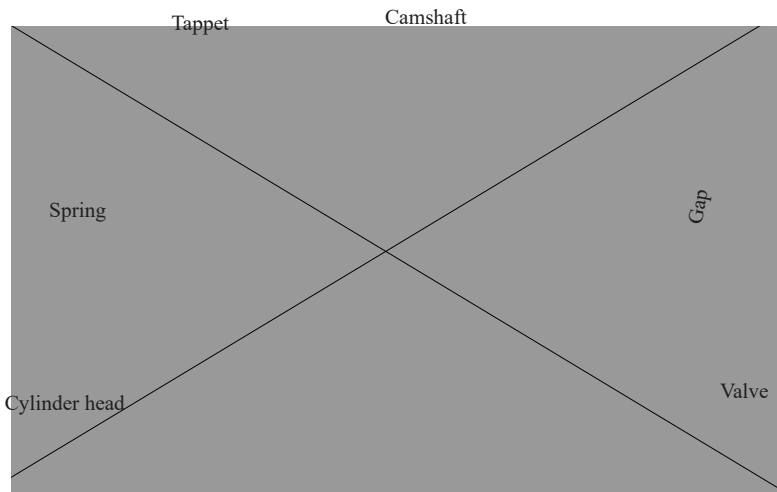

Figure 1. Valve gap assembly

This gap is either too large or too small, will affect the engines' operating parameters, such as air intake and discharge and sealing. And then, engine performance, i.e., torque, oil consumption, and NVH, are affected. Figure 2 shows the experimental data for an engine, which illustrates the influence of valve clearance variation on torque.
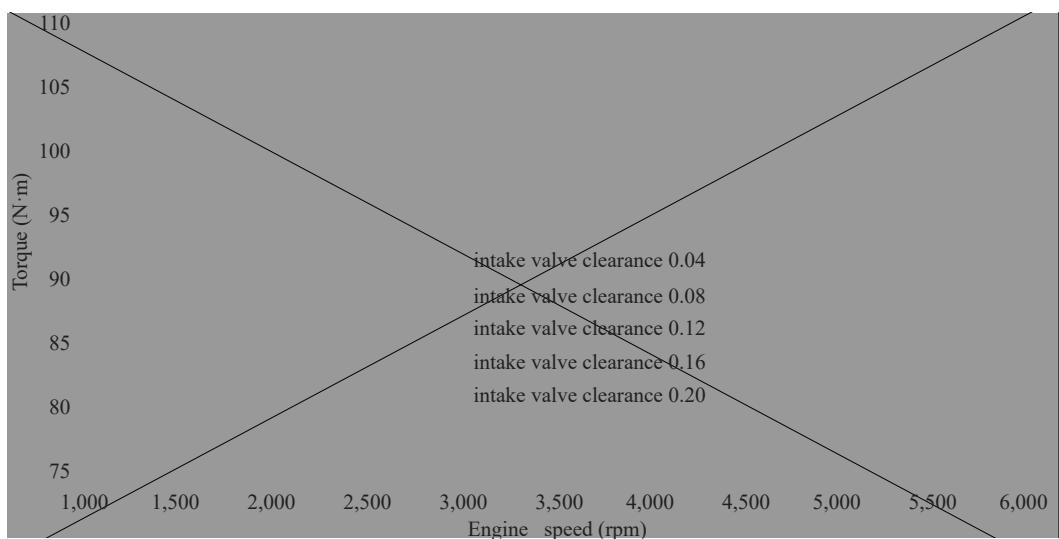

Figure 2. The influence of valve clearance variation on torque

Engineering Science & Technology

The gap is determined by the engines' functional requirement (FR). Its tolerance is the accumulation of tolerances of all components. Therefore, tolerance analysis and allocation for the valve mechanism are important. As we know, there are many geometric tolerances specified on the cam, valve, tappet, and cylinder head, such as parallelism and perpendicularity tolerances. They are represented and transferred in 3D space. Traditional one- or two-dimensional tolerance analysis models cannot effectively deal with geometric tolerances. In the last few years, 3D tolerance analysis methods have been developed gradually [12]. These are innovative technologies that represent and transfer tolerance in 3D Euclidean space. Geometric and dimensional tolerances, as well as the interaction between them, can be taken into consideration by these methods [13]. Typical 3D tolerance analysis models include the T-Map model [14], matrix model [15], direct linear method (DLM) [16], skin model [17], and unified Jacobian-Torsor model [18]. They are reported largely and studied deeply in the literature [19], [20]. Among them, the unified Jacobian-Torsor model uses the Torsor model for tolerance representation and the Jacobian matrix for tolerance propagation. Both deterministic and statistical analysis methods for this model are concise and efficient. Moreover, the tolerance allocation of this model has been studied preliminarily. For complex assemblies containing a large number of geometric tolerances, such as the valve mechanism, the unified Jacobian-Torsor model may be more suitable theoretically.

In this paper, based on the unified Jacobian-Torsor model, 3D tolerance analysis and allocation for the valve gap of engines are presented. For the special conical structure in the valve mechanism, the expression and variation of conical torsor were deduced. At last, a real engine was selected as an example of the analysis process. Sufficient comparison and discussion were made for the results, which demonstrated the effectiveness of the method.

The rest of the paper is organized as follows. Section 2 provides a review of the unified Jacobian-Torsor model and deduces the expression and variation of the conical torsor. Section 3 illustrates this method with a real engine. Section 4 is the comparison and discussion. Section 5 is the conclusion.

2. Unified Jacobian-Torsor model

The unified Jacobian-Torsor model is composed of the Torsor model and the Jacobian matrix. The torsor model uses three translational vectors and three rotational vectors to represent the position and orientation of an ideal surface or its features (axis, center, plane) in relation to another ideal surface in a kinematic manner. These vectors are transferred to the FR using the Jacobian matrix. Jacobian matrices describe relative positions between local reference frames and the FR's one, and relative orientations between local reference frames and the global one. The Torsor model is suitable for tolerance representation, whereas the Jacobian matrix is good at tolerance propagation. The final expression of the unified Jacobian-Torsor model can be written as follows:

$$
\begin{bmatrix}
(\underline{u},\overline{u}) \\
(\underline{v},\overline{v}) \\
(\underline{w},\overline{w}) \\
(\underline{\alpha},\overline{\alpha}) \\
(\underline{\beta},\overline{\beta}) \\
(\underline{\gamma},\overline{\gamma})
\end{bmatrix}_{FR}
= \begin{bmatrix} [J]_{FE1} & \cdots & [J]_{FEn} \end{bmatrix} \times
\begin{bmatrix}
\begin{bmatrix}
(\underline{u},\overline{u}) \\
(\underline{v},\overline{v}) \\
(\underline{w},\overline{w}) \\
(\underline{\alpha},\overline{\alpha}) \\
(\underline{\beta},\overline{\beta}) \\
(\underline{\gamma},\overline{\gamma})
\end{bmatrix}_{FE1}
& \cdots &
\begin{bmatrix}
(\underline{u},\overline{u}) \\
(\underline{v},\overline{v}) \\
(\underline{w},\overline{w}) \\
(\underline{\alpha},\overline{\alpha}) \\
(\underline{\beta},\overline{\beta}) \\
(\underline{\gamma},\overline{\gamma})
\end{bmatrix}_{FEn}
\end{bmatrix}^{T}
\tag{1}
$$

Where FE is the functional element; α, β, and γ indicate the vectors around the axes x, y, and z in the local reference system, respectively; u, v, and w are three specific vectors along the axes x, y, and z, respectively. $(\underline{u}, \overline{u})$ is the tolerance interval where u must lie, and other vectors follow the same way.

Originally, the above equation was calculated in a deterministic way. A statistical method for the unified Jacobian-Torsor model has been proposed by Ghie et al. [21]. The intervals in equation (1) become constraints for the generation of random values for each component in every torsor. Monte Carlo simulation is used to take all random values into

computation. Chen et al. [10] introduced a modified statistical method in which the relation of six vectors in FEs constrained by tolerances was considered.

The tolerance allocation of this model in a deterministic way has been studied by Ghie et al. [22]. By virtue of the data fitting algorithm, Chen et al. [23] proposed a statistical method of distinguishing and quantifying tolerances for this model, where tolerance allocation was carried out according to the contribution of each tolerance.

The analysis objects in the above literature about the unified Jacobian-Torsor model are common features, i.e., shaft, hole, and plane. However, there are special features, such as conical and spiral features, in some assemblies. As shown in Figure 1, valve sealing is completed by the conical fit between the valve and the cylinder head. In fact, because of its coaxial and self-holding properties and well sealability, the conical feature is widely used in machines and mechanisms. In addition to the valve mechanism, the conical feature is also found in bearings and tools. Therefore, it is necessary to incorporate the conical feature into the unified Jacobian-Torsor model.

2.1 *Conical feature*

As we know, a rigid part has six degrees of freedom (DOF) in space. Similarly, a feature has one to six DOFs in the tolerance zone. The number of DOFs depends on the type of feature and tolerance. A conical feature constrained by tolerance has only one DOF. As shown in Figure 3, the torsor of a conical feature can be written as follows:

$$T_C = \left[\left(\underline{u},\ \overline{u} \right)\ \left(\underline{v},\ \overline{v} \right)\ \left(\underline{w},\ \overline{w} \right)\ \left(\underline{\alpha},\ \overline{\alpha} \right)\ \left(\underline{\beta},\ \overline{\beta} \right)\ \left(\text{null} \right) \right]^{T} \tag{2}$$
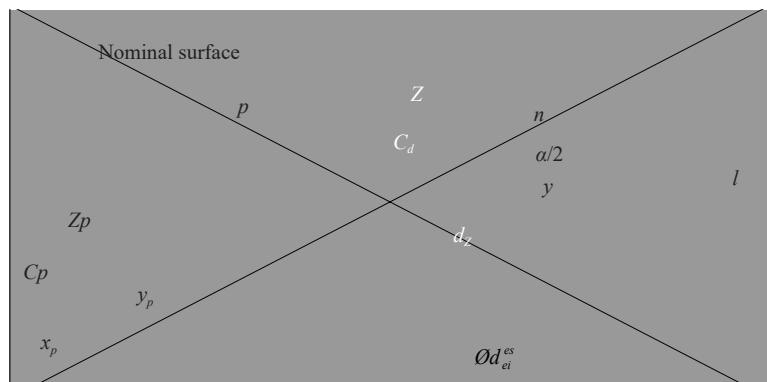

Figure 3. Tolerance and frame of conical feature

Where null indicates that the rotational vector around the conical axis is meaningless for the tolerance representation of the conical torsor.

The above equation lists the general expression of a conical feature. The relationship between the vectors is not stated. According to the tolerancing principle, all components cannot arrive at their limited values at the same time. Obviously, γ and β must shrink to zero when u reaches its maximum value.

Figure 3 shows the tolerance zone of a conical surface specified with a size tolerance at the big end. The local coordinate system is constructed where the z-axis is parallel to the axis of the cone. We have the geometric relation:

$$\left(d_z + ei \right) / 2 \le \left| C_d \times \left(P - C_P \right) \right| \le \left(d_z + es \right) / 2 \tag{3}$$

where C_d and C_p are the orientation and location vector of the size tolerance zone; es and ei are the upper and lower bound values of the size tolerance; P is the location vector of any point at the tolerance zone. d_z is the diameter of the cone at any section, and the expression is:

$$d_Z = 2 \times \tan(\alpha / 2) \tag{4}$$

Where α is the angle of the conical feature.

If the local coordinate system is located at the midpoint of the conical axis. Then $C_d = [0\ 0\ 1]^T$ and $C_p = 0$. With equations (3) and (4), we have the constraint relations about vectors of the conical torsor with a size tolerance:

$$z \times \tan(\alpha/2) + ei/2 \leq \sqrt{\left(z \times \tan(\alpha/2) + u + z \times \beta\right)^2 + \left(z \times \tan(\alpha/2) + v + z \times \alpha\right)^2} \leq z \times \tan(\alpha/2) + es/2 \quad (5)$$

The variations are:

$$-\frac{es - ei}{2l \times \cos(\alpha/2)} \leq \alpha \leq \frac{es - ei}{2l \times \cos(\alpha/2)} \quad (6)$$

$$-\frac{es - ei}{2l \times \cos(\alpha/2)} \leq \beta \leq \frac{es - ei}{2l \times \cos(\alpha/2)} \quad (7)$$

$$ei \leq u \leq es \quad (8)$$

$$ei \leq v \leq es \quad (9)$$

$$ei \times ctg(\alpha/2) \leq w \leq es \times ctg(\alpha/2) \quad (10)$$

Other tolerances, such as profile and positional tolerances, have similar variations and constraint relations with the size tolerance.

2.2 Conical fit

In reality, a pair of matching cones can form a clearance or interference fit, which depends on their relative position along the axial direction. The axial position is usually controlled by step planes.
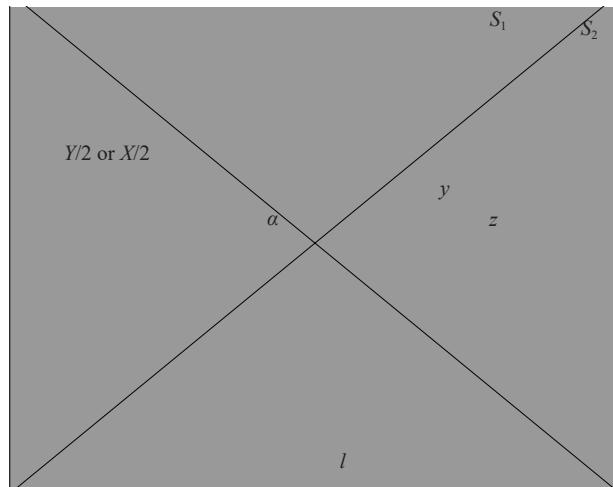

Figure 4. Tolerance and frame of conical fit

Figure 4 shows a clearance fit, where the measuring plane (S_2) of the outer cone is located to the right of the plane of the inner cone (S_1). The value of clearance is X, which can be written as follows:

$$X = |D_{max} - d_{min}| \tag{11}$$

Where D_{max} is the upper limit dimension of the inner cone at any section, while d_{min} is the lower limit dimension of the outer cone at the same section as the inner cone.

And then, the variation of the three translational vectors is $\{-X/2 \leq u \leq X/2; -X/2 \leq v \leq X/2; -\frac{X}{2} \times ctg(\alpha/2) \leq w \leq \frac{X}{2} \times ctg(\alpha/2)\}$, while the variation of the two rotational vectors is $\{-X/2l \leq \alpha \leq X/2l; -X/2l \leq \beta \leq X/2l;$ null$\}$.

Similarly, an interference fit is formed when S_2 is moved to the left of S_1. The valve of interference is Y, which is equal to X in equation (11). Their vector variation is obtained by replacing X with Y.

3. Tolerance analysis and allocation for the valve gap

In this section, a typical gasoline engine is selected to illustrate the 3D tolerance analysis and allocation for the valve gap in detail.

The structure of the valve gap is shown in Figure 1. In fact, the cylinder head includes three parts, i.e., cylinder head, valve seat, and guide. As shown in Figure 5, the valve seat and guide will be pre-pressed into the cylinder head and manufactured together to ensure their positional accuracy. The tolerances of parts and local frames are listed in Table 1.
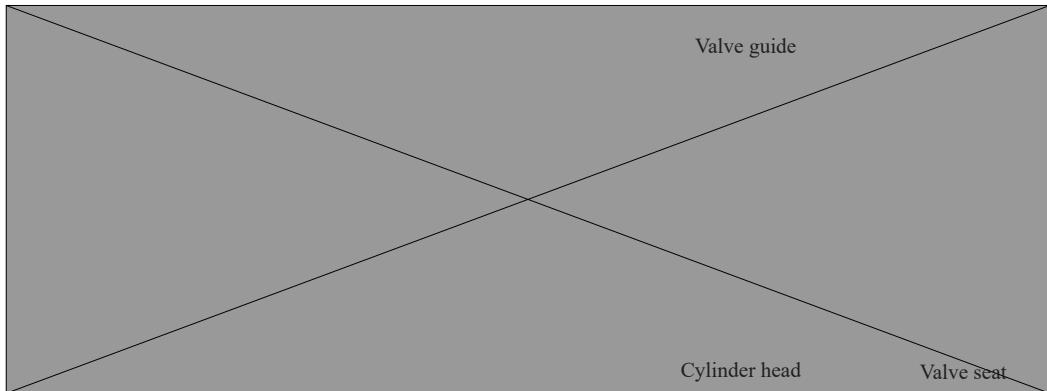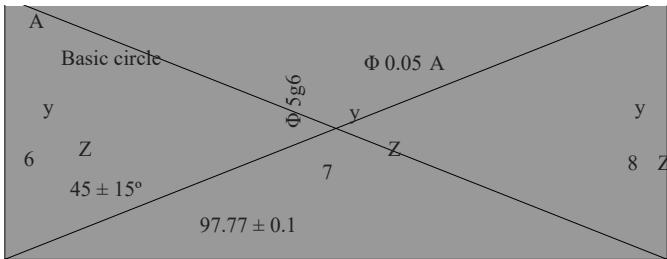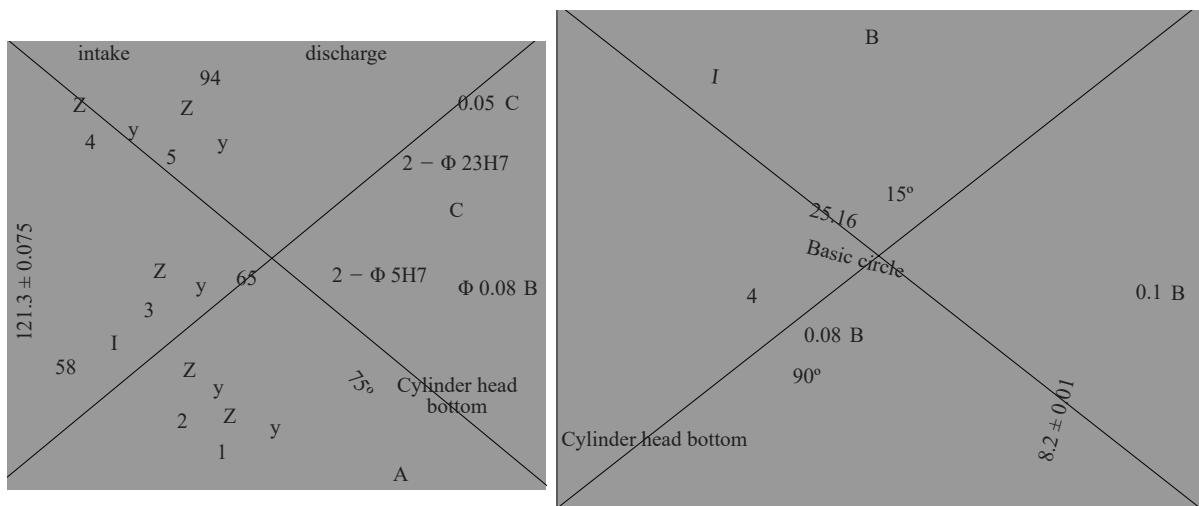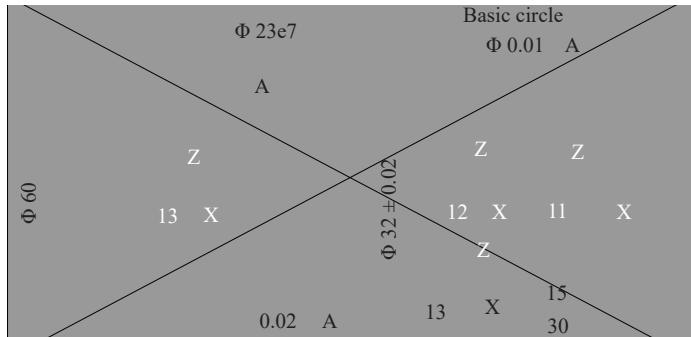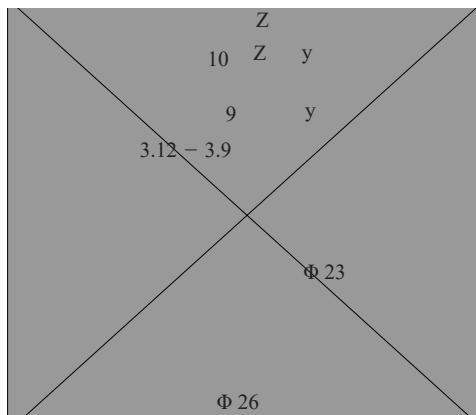

Figure 5. Detailed structure of cylinder head

As shown in Figure 6, the dimension and tolerance of the valve gap are 0.1 and ± 0.025, respectively. The requirement tolerance is stringent, which is the result of the sum of all relative parts' tolerances. This means that each tolerance of part is very small, which is adverse for manufacturing and cost control. Therefore, it is necessary to adopt a special assembly method to balance the quality and cost.

In the actual assembly, the adjustment method is used to meet the requirements of economic production. Specifically, the thickness of the tappet is divided into 40 groups with 0.02-mm intervals. At the end of the assembly process, the corresponding tappet is selected by implementing online measurement and calculation, as shown in Figure 7.

Table 1. Parts' tolerance and local frame

| Part	Tolerance and frame
valve	A Basic circle Φ 0.05 A Φ5g6 y y y 6 Z 7 Z 8 Z 45 ± 15º 97.77 ± 0.1
cylinder head	intake discharge 94 Z Z 0.05 C 4 y 5 y 2 − Φ 23H7 C 121.3 ± 0.075 Z y 65 2 − Φ 5H7 Φ 0.08 B 3 I 58 Z y Cylinder head bottom 75º 2 Z y 1 A — B I 15º 25.16 Basic circle 4 0.1 B 0.08 B 90º 8.2 ± 0.01 Cylinder head bottom
cam	Φ 23e7 Basic circle Φ 0.01 A A Z Z Φ 60 Z 13 X Φ 32 ± 0.02 12 X 11 X Z 0.02 A 13 X 15 30
tappet	Z 10 Z y 9 y 3.12 − 3.9 Φ 23 Φ 26
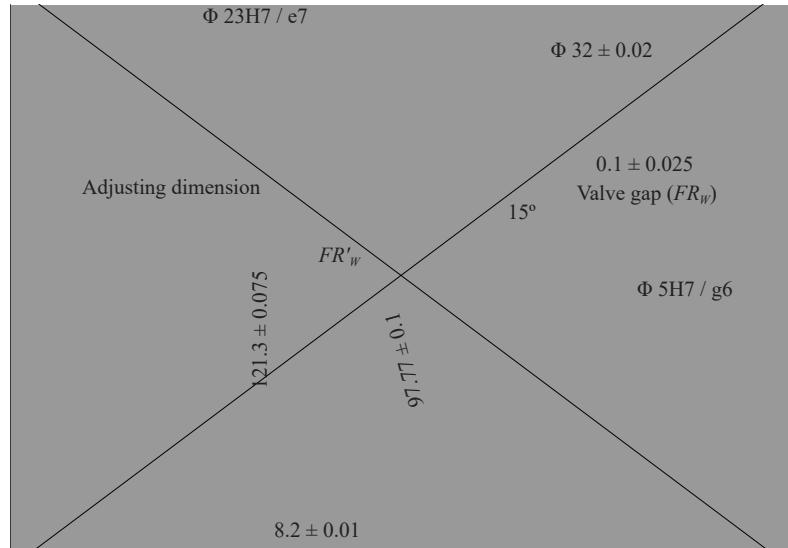
**Figure 6.** Dimensional chain of valve gap
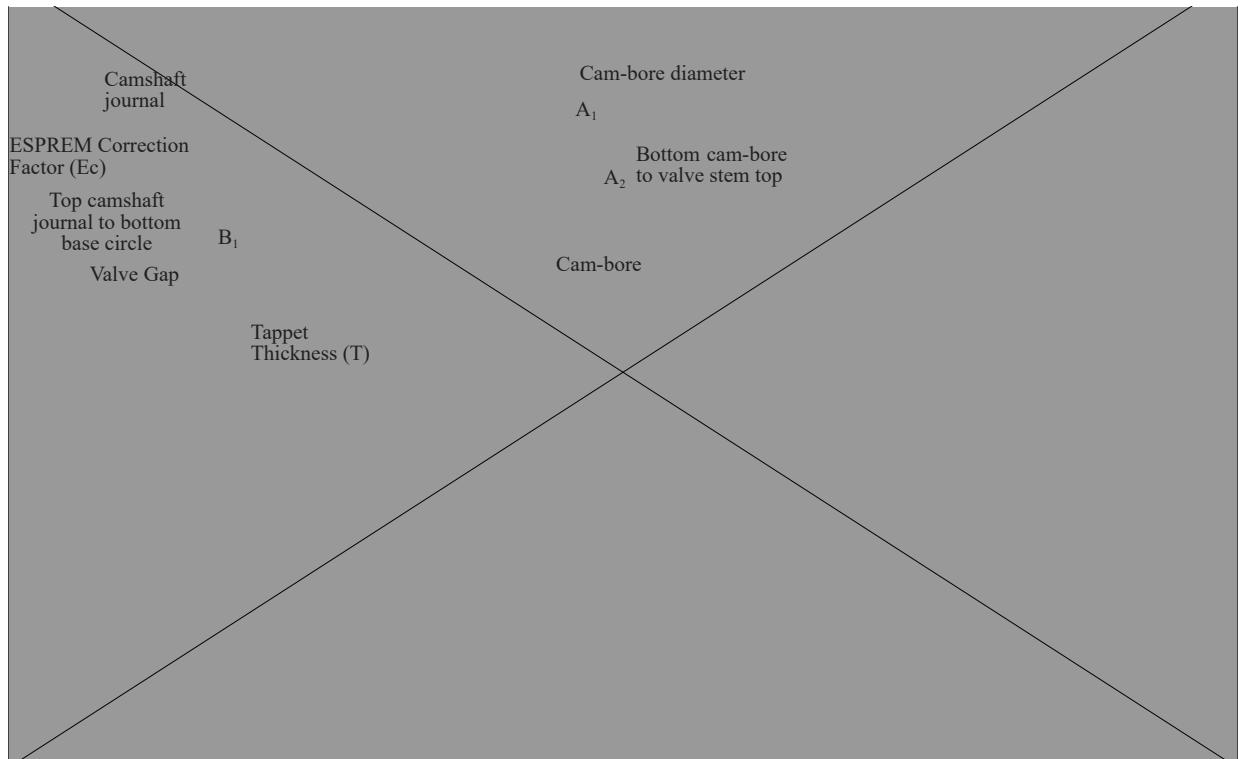
Figure 7. Measurement and calculation of tappet

3.1 *Tolerance analysis*

Based on the assembly process mentioned above, the tolerance transfer route of the valve gap can be drawn as Figure 8, where *FR* is the valve gap. There is a series route, i.e., IFE1-CFE2-IFE3-CFE4-IFE5-FR-IFE6-IFE7-CFE8-IFE9, which is the main transfer route. Besides, there are two partial parallel routes. The first route is PFE1-PFE2-PFE3-CFE2, which is formed by the shoulders of the cam and cylinder head. Another one is PFE4-PFE5-PFE6-CFE8, which

is formed by the valve and the cylinder head.
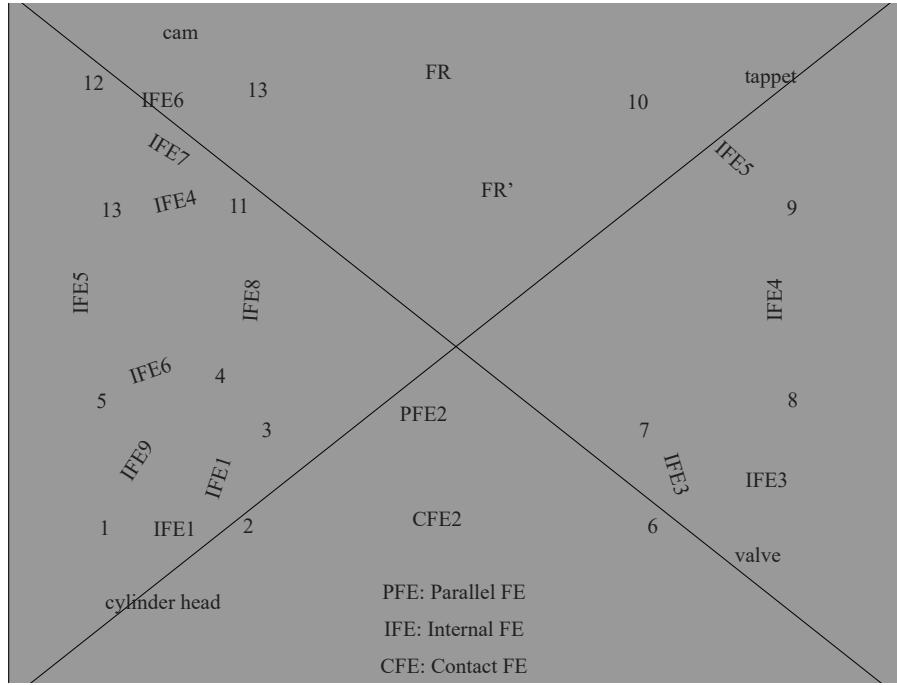
Figure 8. Transfer route of valve gap

When the valve is assembled to the cylinder head, the FR' in Figure 8 is obtained by measurement and calculation. Then, a particular tappet is selected to form the right valve gap. According to the introduction in section 2, the FEs and their variations are listed in Table 2. It should be noted that CFE2 is 0 because the conical fit between the valve and valve seat is stuck together by springs. CFE4 is the same situation where two planes of valve and tappet stick together.

In order to calculate convenience, PFEs in two partial parallel routes can be transformed by Boolean operation [11]. Therefore, we can use FE2' to replace PFE1-PFE2-PFE3, and FE8' to replace PFE4-PFE6-CFE8. The two new torsors and their variations can be written as:

$$T_{2'} = T_{PFE1} \bigcup T_{PFE2} \bigcup T_{PFE3} = \begin{bmatrix} u_{2'} & v_{2'} & 0 & \alpha_{2'} & \beta_{2'} & 0 \end{bmatrix}^T \tag{12}$$

$$V_{2'} = V_{PFE1} \prod V_{PFE2} \prod V_{PFE3} = \begin{Bmatrix} -0.035/2 \leq u_{2'} \leq 0.035/2 \\ -0.035/2 \leq v_{2'} \leq 0.035/2 \\ -0.05/196 \leq \alpha_{2'} \leq 0.05/196 \\ -0.05/196 \leq \beta_{2'} \leq 0.05/196 \end{Bmatrix} \tag{13}$$

$$T_{8'} = T_{PFE4} \bigcup T_{PFE6} \bigcup T_{CFE8} = \begin{bmatrix} u_{8'} & v_{8'} & w_{8'} & 0 & \beta_{8'} & \gamma_{8'} \end{bmatrix}^T \tag{14}$$

$$V_{8'} = V_{PFE4} \prod V_{PFE6} \prod V_{CFE8} = \begin{Bmatrix} -0.02/2 \leq u_{8'} \leq 0.02/2 \\ -0.081/2 \leq v_{8'} \leq 0.081/2 \\ -0.081/2 \leq w_{8'} \leq 0.081/2 \\ -0.02/120 \leq \beta_{8'} \leq 0.02/120 \\ -0.02/120 \leq \gamma_{8'} \leq 0.02/120 \end{Bmatrix} \tag{15}$$

Table 2. Torsors and their variations

FE	torsor	variation
IFE1	$\begin{bmatrix} u_1 \\ v_1 \\ w_1 \\ \alpha_1 \\ \beta_1 \\ 0 \end{bmatrix}$	$-0.08/2 \leq u_1 \leq 0.08/2$ $-0.08/2 \leq v_1 \leq 0.08/2$ $-0.01/2 \leq w_1 \leq 0.01/2$ $-0.08/8/\cos45 \leq \alpha_1 \leq 0.08/8/\cos45$ $-0.08/8/\cos45 \leq \beta_1 \leq 0.08/8/\cos45$ $z \times \tan45 - 0.05/2 \leq \sqrt{\left(z \times \tan45 + u_1 + z \times \beta_1\right)^2 + \left(z \times \tan45 + v_1 + z \times \alpha_1\right)^2}$ $\leq z \times \tan45 + 0.05/2$
IFE3	$\begin{bmatrix} 0 \\ 0 \\ w_3 \\ \alpha_3 \\ \beta_3 \\ 0 \end{bmatrix}$	$-0.2/2 \leq w_3 \leq 0.2/2$ $-0.2/5 \leq \alpha_3 \leq 0.2/5$ $-0.2/5 \leq \beta_3 \leq 0.2/5$ $-0.2 \leq (\alpha_3 \times y + \beta_3 \times x) \leq 0.2$ $-0.1 \leq (w_3 + \alpha_3 \times y + \beta_3 \times x) \leq 0.1$
IFE6	$\begin{bmatrix} 0 \\ v_6 \\ w_6 \\ 0 \\ \beta_6 \\ \gamma_6 \end{bmatrix}$	$-0.04/2 \leq v_6 \leq 0.04/2$ $-0.04/2 \leq w_6 \leq 0.04/2$ $-0.04/2/30 \leq \beta_6 \leq 0.04/2/30$ $-0.04/2/30 \leq \gamma_6 \leq 0.04/2/30$ $(w_6 + \beta_6 \times x)^2 + (v_6 + \gamma_6 \times x)^2 \leq 0.02^2$
IFE7	$\begin{bmatrix} 0 \\ v_7 \\ w_7 \\ 0 \\ \beta_7 \\ \gamma_7 \end{bmatrix}$	$-0.01/2 \leq v_7 \leq 0.01/2$ $-0.01/2 \leq w_7 \leq 0.01/2$ $-0.01/2/30 \leq \beta_7 \leq 0.01/2/30$ $-0.01/2/30 \leq \gamma_7 \leq 0.01/2/30$ $(w_7 + \beta_7 \times x)^2 + (v_7 + \gamma_7 \times x)^2 \leq 0.005^2$
CFE8	$\begin{bmatrix} 0 \\ v_8 \\ w_8 \\ 0 \\ \beta_8 \\ \gamma_8 \end{bmatrix}$	$-0.081/2 \leq v_8 \leq 0.081/2$ $-0.081/2 \leq w_8 \leq 0.081/2$ $-0.081/2/15 \leq \beta_8 \leq 0.081/2/15$ $-0.081/2/15 \leq \gamma_8 \leq 0.081/2/15$ $(w_8 + \beta_8 \times x)^2 + (v_8 + \gamma_8 \times x)^2 \leq 0.0405^2$
IFE9	$\begin{bmatrix} 0 \\ v_9 \\ w_9 \\ 0 \\ \beta_9 \\ \gamma_9 \end{bmatrix}$	$-0.15/2 \leq v_9 \leq 0.15/2$ $-0.15/2 \leq w_9 \leq 0.15/2$ $-0.15/2/15 \leq \beta_9 \leq 0.15/2/15$ $-0.15/2/15 \leq \gamma_9 \leq 0.15/2/15$ $(w_9 + \beta_9 \times x)^2 + (v_9 + \gamma_9 \times x)^2 \leq 0.075^2$
PFE1	$\begin{bmatrix} u_{p1} \\ v_{p1} \\ 0 \\ \alpha_{p1} \\ \beta_{p1} \\ 0 \end{bmatrix}$	$-0.08/2 \leq u_{p1} \leq 0.08/2$ $-0.08/2 \leq v_{p1} \leq 0.08/2$ $-0.08/2/65 \leq \alpha_{p1} \leq 0.08/2/65$ $-0.08/2/65 \leq \beta_{p1} \leq 0.08/2/65$ $(u_{p1} + \beta_{p1} \times z)^2 + (v_{p1} + \beta_{p1} \times z)^2 \leq 0.04^2$

Table 2. (cont.)

FE	torsor	variation
PFE2	$\begin{bmatrix} u_{p2} \\ v_{p2} \\ 0 \\ \alpha_{p2} \\ \beta_{p2} \\ 0 \end{bmatrix}$	$-0.035/2 \le u_{p2} \le 0.035/2$ $-0.035/2 \le v_{p2} \le 0.035/2$ $-0.035/2/65 \le \alpha_{p2} \le 0.035/2/65$ $-0.035/2/65 \le \beta_{p2} \le 0.035/2/65$ $(u_{p2} + \beta_{p2} \times z)^2 + (v_{p2} + \beta_{p2} \times z)^2 \le 0.0175^2$
PFE3	$\begin{bmatrix} u_{p3} \\ v_{p3} \\ 0 \\ \alpha_{p3} \\ \beta_{p3} \\ 0 \end{bmatrix}$	$-0.05/2 \le u_{p3} \le 0.05/2$ $-0.05/2 \le v_{p3} \le 0.05/2$ $-0.05/2/98 \le \alpha_{p3} \le 0.05/2/98$ $-0.05/2/98 \le \beta_{p3} \le 0.05/2/98$ $(u_{p3} + \beta_{p3} \times z)^2 + (v_{p3} + \beta_{p3} \times z)^2 \le 0.025^2$
PFE4	$\begin{bmatrix} u_{p4} \\ 0 \\ 0 \\ 0 \\ \beta_{p4} \\ \gamma_{p4} \end{bmatrix}$	$-0.02/2 \le u_{p4} \le 0.02/2$ $-0.02/60/2 \le \beta_{p4} \le 0.02/60/2$ $-0.02/60/2 \le \gamma_{p4} \le 0.02/60/2$ $-0.02 \le (\beta_{p4} \times z + \gamma_{p4} \times y) \le 0.02$
PFE6	$\begin{bmatrix} u_{p6} \\ 0 \\ 0 \\ 0 \\ \beta_{p6} \\ \gamma_{p6} \end{bmatrix}$	$-0.05/2 \le u_{p6} \le 0.05/2$ $-0.05/60 \le \beta_{p6} \le 0.05/60$ $-0.05/60 \le \gamma_{p6} \le 0.05/60$ $-0.05 \le (\beta_{p6} \times z + \gamma_{p6} \times y) \le 0.05$ $-0.025 \le (u_{p6} + \beta_{p6} \times z + \gamma_{p6} \times y) \le 0.025$

As can be seen in Figure 8, FR' is the difference of positive (FR'_1) and negative (FR'_2) directions. FR'_1 is composed of IFE1, FE2', and IFE3, while FR'_2 consists of IFE5, IFE7, FE8', and IFE9. The frames are shown in Table 1, and the two Jacobian matrices are:

$$J_{FR'_1} = \begin{bmatrix} \begin{bmatrix} 1 & 0 & 0 & 0 & 97.77 & -26.20 \\ 0 & 1 & 0 & -97.77 & 0 & 0 \\ 0 & 0 & 1 & 26.20 & 0 & 0 \\ 0 & 0 & 0 & 1 & 0 & 0 \\ 0 & 0 & 0 & 0 & 1 & 0 \\ 0 & 0 & 0 & 0 & 0 & 1 \end{bmatrix}_{IFE1} \begin{bmatrix} 1 & 0 & 0 & 0 & 97.77 & -26.20 \\ 0 & 1 & 0 & -97.77 & 0 & 0 \\ 0 & 0 & 1 & 26.20 & 0 & 0 \\ 0 & 0 & 0 & 1 & 0 & 0 \\ 0 & 0 & 0 & 0 & 1 & 0 \\ 0 & 0 & 0 & 0 & 0 & 1 \end{bmatrix}_{FE2'} \begin{bmatrix} 1 & 0 & 0 & 0 & 0 & 0 \\ 0 & 1 & 0 & 0 & 0 & 0 \\ 0 & 0 & 1 & 0 & 0 & 0 \\ 0 & 0 & 0 & 1 & 0 & 0 \\ 0 & 0 & 0 & 0 & 1 & 0 \\ 0 & 0 & 0 & 0 & 0 & 1 \end{bmatrix}_{IFE3} \end{bmatrix} \quad (16)$$

$$J_{FR'_2} = \begin{bmatrix} \begin{bmatrix} 1 & 0 & 0 & 0 & 0 & 0 \\ 0 & 1 & 0 & 0 & 0 & 0 \\ 0 & 0 & 1 & 0 & 0 & 0 \\ 0 & 0 & 0 & 1 & 0 & 0 \\ 0 & 0 & 0 & 0 & 1 & 0 \\ 0 & 0 & 0 & 0 & 0 & 1 \end{bmatrix}_{IFE6} \begin{bmatrix} 1 & 0 & 0 & 0 & -16 & 4.29 \\ 0 & 1 & 0 & 16 & 0 & 0 \\ 0 & 0 & 1 & -4.29 & 0 & 0 \\ 0 & 0 & 0 & 1 & 0 & 0 \\ 0 & 0 & 0 & 0 & 1 & 0 \\ 0 & 0 & 0 & 0 & 0 & 1 \end{bmatrix}_{IFE7} \begin{bmatrix} 1 & 0 & 0 & 0 & -16 & 4.29 \\ 0 & 1 & 0 & 16 & 0 & 0 \\ 0 & 0 & 1 & -4.29 & 0 & 0 \\ 0 & 0 & 0 & 1 & 0 & 0 \\ 0 & 0 & 0 & 0 & 1 & 0 \\ 0 & 0 & 0 & 0 & 0 & 1 \end{bmatrix}_{FE8'} \begin{bmatrix} 1 & 0 & 0 & 0 & -16 & 4.29 \\ 0 & 1 & 0 & 16 & 0 & 0 \\ 0 & 0 & 1 & -4.29 & 0 & 0 \\ 0 & 0 & 0 & 1 & 0 & 0 \\ 0 & 0 & 0 & 0 & 1 & 0 \\ 0 & 0 & 0 & 0 & 0 & 1 \end{bmatrix}_{IFE9} \end{bmatrix} \quad (17)$$

With equation (1), a statistical method is used to calculate the result by virtue of the Monte Carlo simulation. The calculating process is completed by Matlab®. In order to ensure the accuracy, the number of iterations was set to 10,000. Here we only pay attention to the gap, i.e., w in FR', which is the distance between the top plane of the valve and the bottom of the basic circle of the cam (as shown in Figure 6). The statistical results of $\sigma_{FR'_{1w}} = 0.0346$ and $\sigma_{FR'_{2w}} = 0.0278$. And then, w' is the sum of the two obtained results.

$$\sigma_{FR'_w} = \sqrt{\sigma^2_{FR'_{1w}} + \sigma^2_{FR'_{2w}}} = 0.0444 \tag{18}$$

According to the dimensions of the cylinder head, cam, and valve, the basic dimension of FR' is 3.609. Therefore, $FR_w = 3.609 \pm 3 \times 0.0444 = 3.609 \pm 0.1332$.

3.2 *Tolerance allocation*

As mentioned above, the tappet is an adjusting part, which is selected in line with the difference of FR_w and $FR_{w'}$. The tolerance of the tappet is ± 0.01. The compensation value of the tappet is $F = 0.2664$ (2×0.1332), and the compensation ability is $S = 2 \times (0.025 - 0.01)$. The number of groups of tappet Z is obtained by the following function.

$$Z = F / S + 1 = 0.2664 / 0.03 + 1 = 9.88 \tag{19}$$

Rounding the results, we can get that the final grouping number of the vertical column should be 10 groups, as shown in Table 3.

Table 3. Groups of tappets

No	The thickness of the tappet	The distance between the top plane of the valve and the bottom of the basic circle of the cam	Valve gap
1	3.364-3.384	3.476-3.489	0.092-0.125
2	3.394-3.414	3.489-3.519	0.075-0.125
3	3.424-3.444	3.519-3.549	0.075-0.125
4	3.454-3.474	3.549-3.579	0.075-0.125
5	3.484-3.504	3.579-3.609	0.075-0.125
6	3.514-3.534	3.609-3.639	0.075-0.125
7	3.544-3.564	3.639-3.669	0.075-0.125
8	3.574-3.694	3.669-3.699	0.075-0.125
9	3.604-3.624	3.699-3.729	0.075-0.123
10	3.634-3.654	3.729-3.742	0.075-0.108

The first and last groups compress the tolerance of the valve gap because there is a rounding process in calculation. This is unavoidable in the adjusting method of assembly. Meanwhile, the compression of the two groups is very small, and it is on the edge of the column grouping, which is rarely used in theory.

4. Comparison and discussion

In practical production, although the thickness of the tappet is divided into 40 groups with 0.02-mm intervals, only 20 of them, i.e., No 13-32, are available on the assembly line, the thickness of which is 3.35-3.67 mm. The first 12 groups and the last 8 groups are no longer prepared. The results of tolerance analysis and allocation in the previous

section are well consistent with the actual situation.

In addition, 25 engines were selected from the production line to measure the values of the intake valve gap. Each engine has 8 intake valves. The measuring tool is calliper, with a measurement accuracy of ± 0.001 mm. The measuring tool and value are shown in Figure 9.
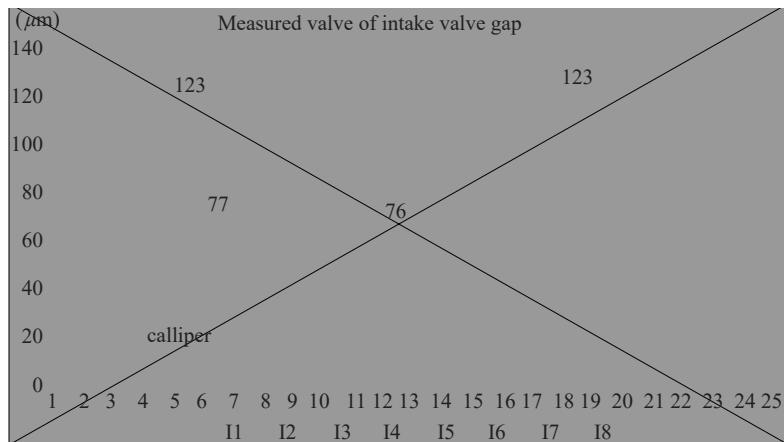

Figure 9. Experimental data

The experimental results confirm that the 3D analysis process and calculation results based on the unified Jacobian-Torsor model are correct.

This engine was designed many years ago. Tolerance analysis and allocation adopt the traditional linear dimensional chain, where many geometric tolerances can not be taken into consideration. The analysis result was not accurate, which directly affects the tolerance allocation. The more groups there are, the higher the cost. In other words, 3D tolerance analysis technology is necessary for accurate tolerance analysis and optimization of complex assemblies, such as engines.

5. Conclusion

Based on the unified Jacobian-Torsor model, the present work attempts to propose a 3D method of tolerance analysis and allocation for valve gaps in engines, where the large geometric and partial parallel connections were taken into consideration. For the special conical structure in the valve mechanism, the expression and variation of conical torsor were deduced. This method was illustrated by a real valve gap in engines. Sufficient comparison and discussion were made for the results, which demonstrated the effectiveness of the method. Moreover, the calculating scheme had a practical reference meaning to other 3D models, such as piston linkage and steering mechanisms in automobiles.

Acknowledgement

Conflict of interest

The authors declare that they have no conflict of interest.

References

[1] Z. He, W. Gong, W. Xie, J. Zhang, G. Zhang, and Z. Hong, "NVH and reliability analyses of the engine with different interaction models between the crankshaft and bearing," *Applied Acoustics*, vol. 101, no. 1, pp. 185-200, 2016.

[2] S. Yang, Z. Ma, X. Li, D. L. S. Hung, and M. Xu, "A review on the experimental non-intrusive investigation of fuel injector phase changing flow," *Fuel*, vol. 259, no. 1, pp. 116188, 2020.

[3] M. Javidani, and D. Larouche, "Application of cast Al-Si alloys in internal combustion engine components," *International Materials Reviews*, vol. 59, no. 3, pp. 132-158, 2014.

[4] S. Du, L. Xi, J. Ni, P. Ershun, and C. R. Liu, "Product lifecycle-oriented quality and productivity improvement based on stream of variation methodology," *Computers in Industry*, vol. 59, no. 2-3, pp. 180-192, 2008.

[5] Y. S. Hong, and T. C. Chang, "A comprehensive review of tolerancing research," *International Journal of Production Research*, vol. 40, no. 11, pp. 2425-2459, 2002.

[6] Z. Shen, G. Ameta, J. J. Shah, and J. K. Davidson, "A comparative study of tolerance analysis methods," *Journal of Computing and Information Science in Engineering*, vol. 5, no. 3, pp. 247-256, 2005.

[7] K. Wang, G. Li, S. Du, L. Xi, and T. Xia, "State space modelling of variation propagation in multistage machining processes for variable stiffness structure workpieces," *International Journal of Production Research*, vol. 59, no. 13, pp. 4033-4052, 2021.

[8] F. Yang, S. Jin, Z. Li, S. Ding, and X. Ma, "A new error compensation model for machining process based on differential motion vectors," *International Journal of Advanced Manufacturing Technology*, vol. 93, pp. 2943-2954, 2017. Available: https://doi.org/10.1007/s00170-017-0652-z.

[9] D. Xu, J. Bao, and Y. Jin, "Tolerance analysis & tolerance optimization of complex diesel engine key structures," *Computer Integrated Manufacturing Systems*, vol. 12, no. 5, pp. 721-726, 2006.

[10] H. Chen, S. Jin, Z. Li, and X. Lai, "A modified method of the unified Jacobian-Torsor model for tolerance analysis and allocation," *International Journal of Precision Engineering and Manufacturing*, vol. 16, pp. 1789-1800, 2015. Available: https://doi.org/10.1007/s12541-015-0234-7.

[11] H. Chen, S. Jin, Z. Li, and X. Lai, "A solution of partial parallel connections for the unified Jacobian-Torsor model," *Mechanism and Machine Theory*, vol. 91, pp. 39-49, 2015. Available: https://doi.org/10.1016/j.mechmachtheory.2015.03.012.

[12] C. Bo, Z. Yang, L. Wang, and H. Chen, "A comparison of tolerance analysis models for assembly," *International Journal of Advanced Manufacturing Technology*, vol. 68, pp. 739-754, 2013. Available: https://doi.org/10.1007/s00170-013-4795-2.

[13] H. Chen, S. Jin, Z. Li, and X. Lai, "A comprehensive study of three dimensional tolerance analysis methods," *Computer-Aided Design*, vol. 53, pp. 1-13, 2014. Available: https://doi.org/10.1016/j.cad.2014.02.014.

[14] J. K. Davidson, A. Mujezinovic, and J. J. Shah, "A new mathematical model for geometric tolerances as applied to round faces," *Journal of Mechanical Design*, vol. 124, no. 4, pp. 609-622, 2002.

[15] A. Desrochers, and A. Riviere, "A matrix approach to the representation of tolerance zones and clearances," *International Journal of Advanced Manufacturing Technology*, vol. 13, pp. 630-636, 1997. Available: https://doi.org/10.1007/BF01350821.

[16] K. W. Chase, J. Gao, and S. P. Magleby, "General 2-D tolerance analysis of mechanical assemblies with small kinematic adjustments," *Journal of Design and Manufacturing*, vol. 5, pp. 263-274, 1995.

[17] B. Schleich, N. Anwer, L. Mathieu, and S. Wartzack, "Skin Model Shapes: A new paradigm shift for geometric variations modelling in mechanical engineering," *Computer-Aided Design*, vol. 50, pp. 1-15, 2014. Available: https://doi.org/10.1016/j.cad.2014.01.001.

[18] A. Desrochers, W. Ghie, and L. Laperriere, "Application of a unified Jacobian-Torsor model for tolerance analysis," *Journal of Computing and Information Science in Engineering*, vol. 3, no. 1, pp. 2-14, 2003.

[19] M. Marziale, and W. Polini, "A review of two models for tolerance analysis of an assembly: Jacobian and torsor," *International Journal of Computer Integrated Manufacturing*, vol. 24, no. 1, pp. 74-86, 2011.

[20] M. Marziale, and W. Polini, "A review of two models for tolerance analysis of an assembly: Vector loop and

matrix," *International Journal of Advanced Manufacturing Technology*, vol. 43, pp. 1106-1123, 2009. Available: https://doi.org/10.1007/s00170-008-1790-0.

[21] W. Ghie, L. Laperriere, and A. Desrochers, "Statistical tolerance analysis using the unified Jacobian-Torsor model," *International Journal of Production Research*, vol. 48, no. 15, pp. 4609-4630, 2010.

[22] W. Ghie, L. Laperrière, and A. Desrochers, *Re-Design of Mechanical Assemblies using the Unified Jacobian-Torsor Model for Tolerance Analysis*. Springer Netherlands, 2007.

[23] H. Chen, X. Li, and S. Jin, "A statistical method of distinguishing and quantifying tolerances in assemblies," *Computers & Industrial Engineering*, vol. 156, pp. 107259, 2021. Available: https://doi.org/10.1016/j.cie.2021.107259.